

ON SPACE AND TIME STEP SIZES IN ULTRASONIC PULSE PROPAGATION MODELLING

Rimantas Barauskas

Engineering Mechanics Department
Kaunas University of Technology, Kaunas, Lithuania
e-mail : rimantas.barauskas@mf.ktu.lt

Key words: computational ultrasonics, acoustics, transient dynamics, numerical integration, combined mass matrices, accuracy

Abstract. The focus of the work is to analyse and improve the accuracy of space and time discretized rectangular finite element models for transient acoustic and elastic wave propagation. The propagation of the typical ultrasonic pulse excited on the boundary of the environment is under investigation. The dispersion relations of finite element models have been significantly improved by selecting appropriate form of the mass matrix. As a consequence, only 7-8 elements per wavelength of the main harmonic component of the pulse suffice to represent satisfactory the wave propagation law. As contraindication for using such an approach is a non-diagonal form of the mass matrix requiring to use iterative methods for solving the linear algebraic equation system at each time step. However in 2D and 3D cases the increase of the element size results in considerable savings in memory and computational time even if iteration at each time step is necessary. With increased element size the accuracy requirement instead of stability is dominating for the selection of the time step. The explicit time integration schemes in the case of non-diagonal mass matrix have no computational advantage, and implicit ones can be discussed. The performance of several numerical integration schemes has been evaluated in this study. From the point of view of combined performance and accuracy criterion, the 3-rd order generalized Newmark's scheme and time discontinuous Galerkin finite element method have been selected.

1 Introduction

In a wide range of ultrasonic non-destructive testing and measurement applications, the wave propagation law in acoustic or elastic environment is of primary interest. It is necessary for selecting proper topology of ultrasonic transducers, understanding the features of received signals influenced by cracks or internal irregularities in the bodies of investigation, etc. The above mentioned phenomena are described by well-known wave and dynamic elasticity differential equations. However, the computational structural models obtained on the base of them are still challenging because of their huge dimension necessary to represent adequately the shape and time law of the wave the length of which is much smaller than the spatial dimensions of the body.

In this study we focus our attention on transient behaviour of the propagation of the typical ultrasonic pulse excited on the boundary of the environment. During the last decade a huge effort has been made to create the techniques and software able to solve realistic problems of ultrasonic wave propagation. The available publications on the problem present several different approaches. The finite difference schemes able to associate different density and elastic parameters with each grid point, to take into account the boundaries between different materials and arbitrary geometrical shape of the region are referenced in [1]. The approach has been implemented as WAVE2000 computational ultrasonics software able to solve 2D problems in powerful multiprocessor computing environments, as well as, in PC's. The approach is based on efficient algorithms of step-by-step computation of the structural displacements over all the structure and the time interval. 17 mesh points per shortest wavelength have been used, and the time step ensuring the stability of the explicit time-marching scheme has been estimated as

$\Delta t \leq \frac{\Delta x}{\sqrt{v_l^2 + v_t^2}}$, where v_l, v_t - velocities of the longitudinal and shear elastic waves. The stability of

the explicit numerical integration scheme being ensured, the accuracy requirements are usually satisfied as well - with 17 points per wavelength the maximum free vibration frequency represented by the structural model is usually much higher than the highest harmonic component of the wave of interest. The combination of finite difference and finite element approach has been earlier described in [2].

The three-dimensional problems seem to be most realistic to approach by using the boundary integral equation techniques the transient formulations and implementation of which have been mentioned in [3],[4] for acoustic and in [5] for elastic waves. The space and time step requirements are similar as mentioned above for the finite difference approach, however, only surface of the body has to be discretized. Moreover, adaptive meshing can be employed by using refined meshing in the vicinity of geometrical irregularities. The best results can be expected by combining properly the finite element and boundary element approaches. The boundary integral method is very efficient for presenting the homogeneous regions, however, the sources of numerical instabilities, excessive oscillations of the solution and the measures to cope with them at present are not so clearly understood as for the finite element models. On the other hand, the zones containing non-homogeneous materials are much easier to represent by using finite element models.

This work aims to analyse and improve the accuracy of space and time discretized rectangular finite element models for transient acoustic wave propagation. In uniform finite element models containing identical rectangular elements the solution algorithms are very similar to those used in finite difference schemes as no structural matrices are necessary to

assemble and calculation formulae for each grid point can be easily written. On the other hand, it is easy to couple such models with regions described by means of free finite element meshes, as well as, by boundary element models. It has been shown in [6],[7] that dispersion relations of uni-dimensional finite element models can be significantly improved by selecting appropriate form of the mass matrix. As a consequence, only 5-7 elements per wavelength instead of 17 often suffice to represent satisfactory the wave propagation law. As contraindication for using such an approach is a non-diagonal form of the mass matrix requiring to use iterative methods for solving the linear algebraic equation system at each time step. However in 2D and 3D cases more than 3 times increase of the element size result in considerable savings in computational time even if iteration at each time step is necessary. The time step ensuring stability of the explicit numerical integration schemes is also to the same ratio larger because of the lower value of the highest free vibration frequency represented by the model. In the case of coarser meshes the accuracy requirement and not the algorithmic stability is governing the selection of the time step. On the other hand, the explicit time integration schemes in the case of non-diagonal mass matrix have no computational advantage, and implicit ones can be discussed. The performance of several numerical integration schemes is being evaluated in this study.

2 The wave equation and the element size selection

The acoustic wave propagation in region V bounded by boundary S is described by means of the transient scalar wave equation [8]

$$E\nabla^2 u(\mathbf{x},t) - \rho \frac{\partial^2 u}{\partial t^2} = 0, \quad \mathbf{x} \in V, \quad (1)$$

with prescribed boundary conditions

$$\begin{aligned} u(\mathbf{x},t) &= \bar{u}, \quad \mathbf{x} \in S_1 \\ \frac{\partial u(\mathbf{x},t)}{\partial n} &= \bar{q}, \quad \mathbf{x} \in S_2 \end{aligned} \quad (2)$$

$$\text{and initial conditions } u(\mathbf{x},0) = u_0, \quad \dot{u}(\mathbf{x},0) = v_0, \quad (3)$$

where $u(\mathbf{x},t)$ - velocity potential, \mathbf{x} - spatial co-ordinate, t - time, E, ρ - bulk modulus and density of the material, \bar{u}, \bar{q} - prescribed boundary values of the velocity potential and of the component of the velocity normal to the boundary. The wave velocity is $c = \sqrt{\frac{E}{\rho}}$.

The equation of a finite element is obtained on the base of (2),(3),(4) by using Galerkin weighted residual techniques [9]:

$$[\mathbf{M}^e]\{\ddot{\mathbf{U}}^e\} + [\mathbf{K}^e]\{\mathbf{U}^e\} = \{\mathbf{Q}^e(t)\}, \quad (4)$$

where

$$[\mathbf{K}^e] = E \int_{V^e} (\text{grad}[\mathbf{N}])^T (\text{grad}[\mathbf{N}]) dV,$$

$$[\mathbf{M}_c^e] = \rho \int_{V^e} [\mathbf{N}]^T [\mathbf{N}] dV, \quad \{\mathbf{Q}^e\} = \int_{S_2^e} [\mathbf{N}]^T \bar{q} dV$$

are the ‘‘conductivity’’ matrix, mass matrix and excitation vector of the element correspondingly, $[\mathbf{N}]$ - form function matrix of the element. .

The physical meaning of the excitation vector $\{\mathbf{Q}^e\}$ is the prescribed normal velocity on the

boundary S_2^c of the element. Zero normal velocity corresponding to the value $\{Q^c\}=0$ serves as the “natural” boundary condition. Matrix $[M_L^c]$ is the consistent mass matrix of the element. Alternatively, the “lumped” (diagonal) version of the mass matrix $[M_L^c]$ can be used obtained by distributing the mass equally between the nodes of the element. It has been found in [6],[7] that neither of the two matrices is optimum for acoustic, as well as, elastic wave propagation problems, and the linear combination of them can improve significantly the dispersion relations represented by the model. The demonstration of this can be seen in Fig.1,a,b,c, where the family of curves in each figure represent how the values of natural frequencies of the rectangular acoustic region depend upon the mesh refinement expressed by number of points N per side of the rectangular. The natural frequencies presented in Fig.1a correspond to mass matrix $[M^c]=0.75[M_L^c]+0.25[M_L^c]$ exhibit significantly better convergence. As a result, less distortion of the wave shape in rough meshes can be expected.

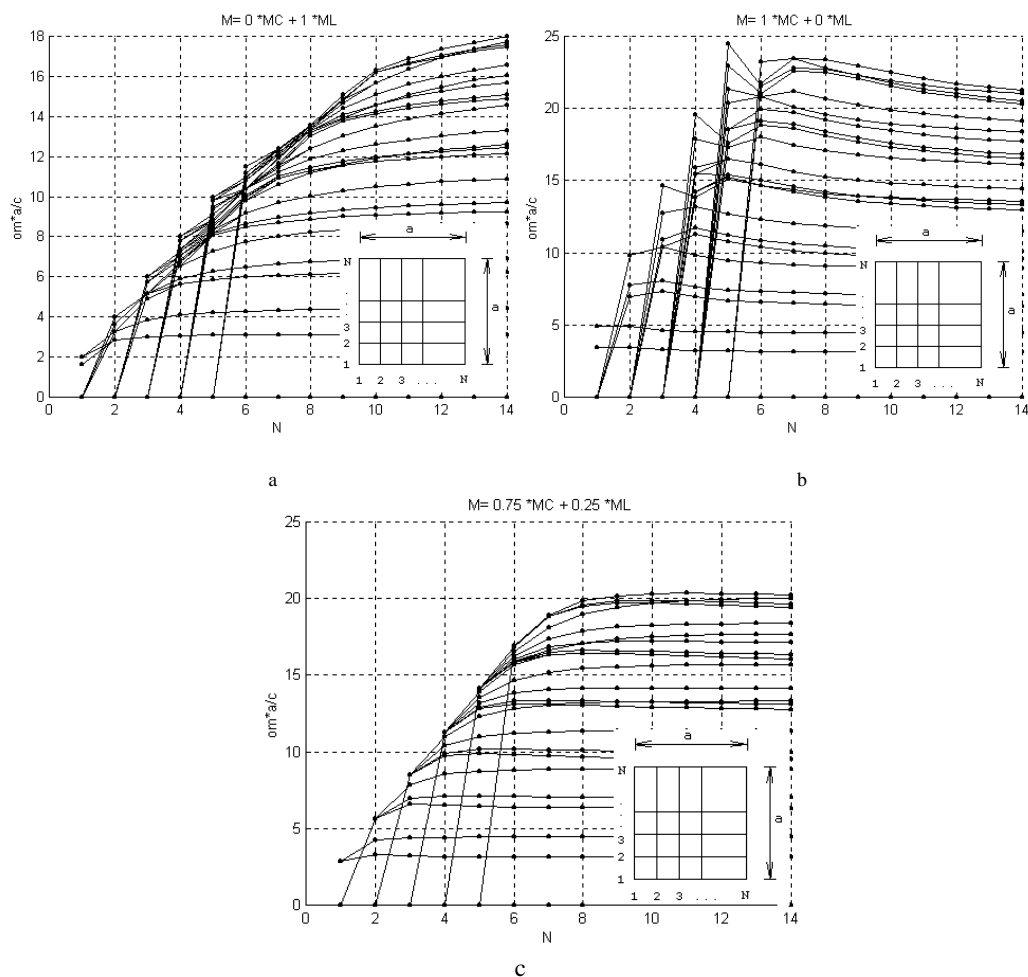


Fig.1 Natural frequencies of hierarchical models of the rectangular acoustic region obtained by using lumped(a), consistent (b) and combined (c) mass matrices

The investigation of the space and time step size in this work has been performed by analysing the ultrasonic pulse propagation excited on the boundary by the input transducer. The time law of the velocity perpendicular to the boundary and its Fourier expansion components is shown in Fig. 2. The width of the spectrum of the pulse in Fig.2b necessary to reproduce the time law in Fig.2a has to contain the harmonic components up to 2.5ω , where ω - the frequency of the main harmonic component of the pulse. By means of numerical experiments it has been shown that the dimension of the element Δx has to satisfy the condition $\frac{c\omega}{\Delta x} > 1.2$ that corresponds to about 7 elements along the wavelength of the main harmonic component. It can be shown that in the case of the lumped mass matrix the condition $\frac{c\omega}{\Delta x} > 5$ has to be satisfied.

Fig.3 presents the shape of the wave propagating along Oy axis and time laws registered by input and output transducers at bottom and top edges of the region correspondingly. Integration time encompasses 2.5 passages of the wave along the vertical left hand side of the region. The wave excited by ultrasonic pulse by the bottom transducer (input) refracts from the top transducer (output) and then one more time from the bottom one. The picture presents converged solution, the convergence being checked by comparison with the solutions in meshes of considerably higher refinement. Fig.4 presents the wave shapes at the moment of refraction from the bottom edge of the domain (time moment $t=2a/c$) obtained by using different element sizes.

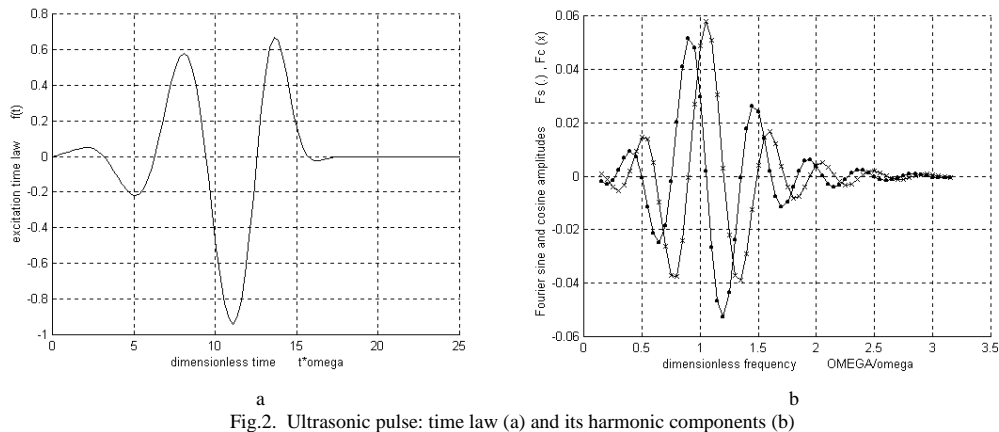


Fig.2. Ultrasonic pulse: time law (a) and its harmonic components (b)

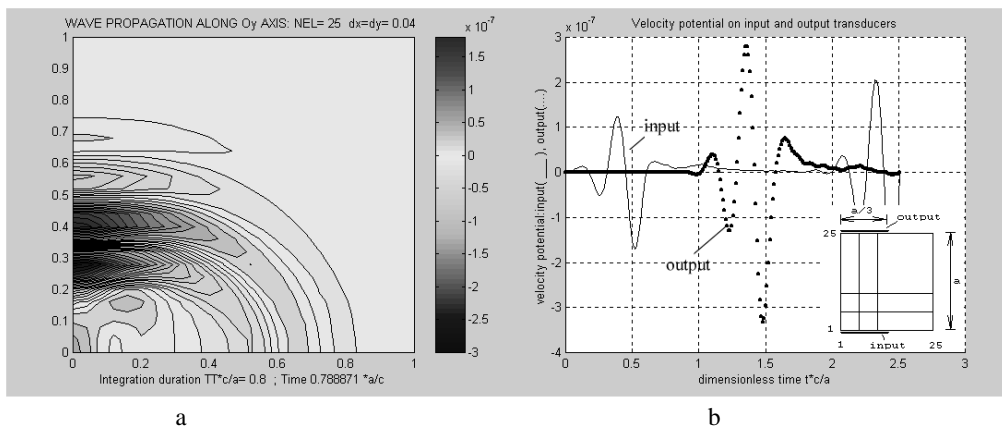


Fig.3 Shape of the wave in terms of the velocity potential propagating in the rectangular region meshed by 25x25 elements (a); Time laws of normal velocity values averaged on input and output transducers (b)

3 Time step selection

Numerous different time integration schemes can be applied for the time integration of the structural wave equation. In the case of the lumped mass matrix the choice is usually restricted to explicit schemes in order to avoid the algebraic matrix equation solution at each time step. As explicit schemes exhibit only conditional stability, the time step size is restricted by the numerical stability condition of the numerical scheme. Practically for the ultrasonic pulse (Fig.2) propagation analysis the time step size is restricted to $\Delta t < \frac{\Delta x}{1.5c}$. As a rule, such time step value is sufficient for ensuring accuracy of the explicit scheme as with $\Delta x = \frac{c\omega}{5}$ we have about 90 integration points per period of the main harmonic component (it is necessary to notice that the highest harmonic component of the pulse taken into account is about 2.5ω , see Fig.2b).

If combined mass matrix is used, the explicit time integration schemes have no computational advantage. Iteration methods for the algebraic matrix equation solution have to be applied in any case, so explicit, as well as, implicit time integration schemes can be used. With larger elements, the time step ensuring the numerical stability of explicit methods is larger and usually this value is too large to ensure accuracy. In other words, accuracy, not the stability, becomes decisive for the selection of the time step.

Here we compare the behaviour of several time integration schemes during the analysis of the ultrasonic pulse propagation and evaluate in each case the maximum possible time integration step. The following time integration schemes have been considered.

Central Difference Scheme (CDS) [10]:

$$\left(\frac{1}{\Delta t^2}[\mathbf{M}] + \frac{1}{2\Delta t}[\mathbf{C}] \right) \{\mathbf{U}_{t+\Delta t}\} = \{\mathbf{Q}_t\} - \left([\mathbf{K}] - \frac{2}{\Delta t^2}[\mathbf{M}] \right) \{\mathbf{U}_t\} - \left(\frac{1}{\Delta t^2}[\mathbf{M}] - \frac{1}{2\Delta t}[\mathbf{C}] \right) \{\mathbf{U}_{t-\Delta t}\};$$

Generalized Newmark's scheme (GNS) [11]:

$$\{\mathbf{q}_k\} = \frac{h^{j-k}}{(j-k)!} \{\mathbf{U}\}_t^{(j)}; \quad b_k = \beta_k \frac{h^{m-k}}{(m-k)!}, \quad k = 0, 1, 2, \dots, m;$$

$$(b_2[\mathbf{M}] + b_1[\mathbf{C}] + b_0[\mathbf{K}]) \Delta \{\mathbf{U}\}^{(m)} = \{\mathbf{Q}_{t+\Delta t}\} - ([\mathbf{M}]\{\mathbf{q}_2\} + [\mathbf{C}]\{\mathbf{q}_1\} + [\mathbf{K}]\{\mathbf{q}_0\}) ,$$

$$\{\mathbf{U}\}_{t+h}^{(k)} = \{\mathbf{q}_k\} + b_k \Delta \{\mathbf{U}\}^{(m)}, \quad k = 0, 1, \dots, m ,$$

where parameters $\beta_k, k = 0, 1, 2, \dots, m$ are selected in order to supply the necessary algorithmic features to the integration scheme;

Modified trapezoidal method (MTM) [13]:

$$[\mathbf{M}](\{\dot{\mathbf{U}}\}_{t+\Delta t} - \{\dot{\mathbf{U}}\}_t) = -[\mathbf{K}]\Delta t \left(\{\mathbf{U}\}_t + \frac{\Delta t}{2} \{\dot{\mathbf{U}}\}_t \right) + \Delta t \{\mathbf{Q}\}_t ;$$

$$\{\mathbf{U}\}_{t+\Delta t} = \{\mathbf{U}\}_t + \frac{\Delta t}{2} (\{\dot{\mathbf{U}}\}_{t+\Delta t} + \{\dot{\mathbf{U}}\}_t);$$

Harmonic acceleration method(HAM) [12]:

$$\begin{aligned} \left([\mathbf{K}] + \frac{a}{\Delta t} [\mathbf{C}] + \frac{b}{\Delta t^2} [\mathbf{M}] \right) \{\mathbf{U}\}_{t+\Delta t} &= \{\mathbf{Q}\}_{t+\Delta t} + \left(\frac{a}{\Delta t} [\mathbf{C}] + \frac{b}{\Delta t^2} [\mathbf{M}] \right) \{\mathbf{U}\}_t + \left(c[\mathbf{C}] + \frac{b}{\Delta t} [\mathbf{M}] \right) \{\dot{\mathbf{U}}\}_t + (d\Delta t[\mathbf{C}] + c[\mathbf{M}]) \{\ddot{\mathbf{U}}\}_t ; \\ \{\dot{\mathbf{U}}\}_{t+\Delta t} &= \frac{a}{\Delta t} (\{\mathbf{U}\}_{t+\Delta t} - \{\mathbf{U}\}_t) - c\{\dot{\mathbf{U}}\}_t - d\Delta t\{\ddot{\mathbf{U}}\}_t ; \\ \{\ddot{\mathbf{U}}\}_{t+\Delta t} &= \frac{b}{\Delta t^2} (\{\mathbf{U}\}_{t+\Delta t} - \{\mathbf{U}\}_t) - \frac{b}{\Delta t} \{\dot{\mathbf{U}}\}_t - c\{\ddot{\mathbf{U}}\}_t ; \\ a &= \frac{\lambda \Delta t}{w} (1 - \cos \lambda \Delta t); b = \frac{\lambda^2 \Delta t^2}{w} \sin \lambda \Delta t; c = \frac{1}{w} (\sin \lambda \Delta t - \lambda \Delta t \cos \lambda \Delta t); \\ d &= \frac{1}{w \lambda \Delta t} (2 - 2 \cos \lambda \Delta t - \lambda \Delta t \sin \lambda \Delta t); w = \lambda \Delta t - \sin \lambda \Delta t ; \end{aligned}$$

where λ is selected close to the frequency of expected main harmonic component of the response;

Time-discontinuous Galerkin finite element method(TDGFEM) [14]:

- 1) $\{\mathbf{Q}_1^*\} = \frac{1}{3} (5\{\mathbf{Q}_1\} + 5[\mathbf{M}]\{\dot{\mathbf{U}}_t^-\} - \{\mathbf{Q}_2\} - 2\Delta t[\mathbf{K}]\{\mathbf{U}_t^-\})$;
 $\{\mathbf{Q}_2^*\} = \{\mathbf{Q}_1\} + \{\mathbf{Q}_2\} + [\mathbf{M}]\{\dot{\mathbf{U}}_t^-\} - \Delta t[\mathbf{K}]\{\mathbf{U}_t^-\}$;
- 2) $\{\dot{\mathbf{U}}_t^{(0)}\} = \{\dot{\mathbf{U}}_t^-\}$; $\{\dot{\mathbf{U}}_{t+\Delta t}^{(0)}\} = \{\dot{\mathbf{U}}_t^-\}$;
- 3) $([\mathbf{M}] + \frac{1}{2} \Delta t[\mathbf{C}] + \frac{1}{6} \Delta t^2[\mathbf{K}])\{\dot{\mathbf{U}}_t^{(i+1)}\} = \{\mathbf{Q}_1^*\} - (\frac{2}{3}[\mathbf{M}] + \frac{1}{6} \Delta t[\mathbf{C}])\{\dot{\mathbf{U}}_{t+\Delta t}^{(i)}\}$;
 $([\mathbf{M}] + \frac{1}{2} \Delta t[\mathbf{C}] + \frac{1}{6} \Delta t^2[\mathbf{K}])\{\dot{\mathbf{U}}_{t+\Delta t}^{(i+1)}\} = \{\mathbf{Q}_2^*\} - (\frac{1}{2} \Delta t[\mathbf{C}] + \frac{1}{3} \Delta t^2[\mathbf{K}])\{\dot{\mathbf{U}}_t^{(i)}\}$;
 $i = 1, 2, \dots$
- 4) $\{\dot{\mathbf{U}}_{t+\Delta t}^-\} = \{\dot{\mathbf{U}}_{t+\Delta t}^{(i)}\}$; $\{\mathbf{U}_{t+\Delta t}^-\} = \{\mathbf{U}_t\} + \frac{1}{2} \Delta t (\{\dot{\mathbf{U}}_t\} + \{\dot{\mathbf{U}}_{t+\Delta t}^{(i)}\})$;

The algorithm enables to apply adaptive time stepping basing on the difference norms $\|\{\dot{\mathbf{U}}_t^-\} - \{\dot{\mathbf{U}}_t\}\|$, $\|\{\mathbf{U}_t^-\} - \{\mathbf{U}_t\}\|$.

We are eager to select the time integration step as large as possible to reduce computational cost and simultaneously to ensure accuracy of the numerical integration. Fig.4 presents the wave shapes at the moment of refraction from the bottom edge of the domain (time moment $t = \frac{2a}{c}$) obtained by means of the above mentioned time integration schemes and compared with the solution obtained with considerably smaller time step which we regard as the "exact" solution. Simple comparison indicates that the best accuracy has been obtained by using third accuracy order GNS with parameters $\beta_0 = \frac{1}{4}$; $\beta_1 = \frac{1}{3}$; $\beta_2 = \frac{1}{2}$; $\beta_3 = 1$ and TDGFEM. However, TDGFEM requires considerably more arithmetic operations at each time step because of the internal iteration loop. It is to be noticed that the selection of the time step size here was determined by accuracy considerations, the conditional algorithmic stability limit being reached at larger values of the time step size. As it can be seen from the results presented in Fig.5, larger time steps are not reasonable to apply.

If more refined mesh is being used, e.g., $\Delta x = \frac{c}{2\omega}$, the time step size is limited by stability considerations. We investigate the situation, when the time step size is beyond the

algorithmic stability limit of conditionally stable schemes. Now unconditionally stable schemes have to be applied, as representatives of which we select HAM and second order unconditionally stable GNS with $\beta_0 = \frac{1}{2}$; $\beta_1 = \frac{1}{2}$; $\beta_2 = 1$. Fig.6 represents the results obtained by using the two schemes and conditionally stable TDGFEM the stability limit of which has not been yet reached by the time step size. The behaviour of the solution obtained by using TDGFEM is obviously the best.

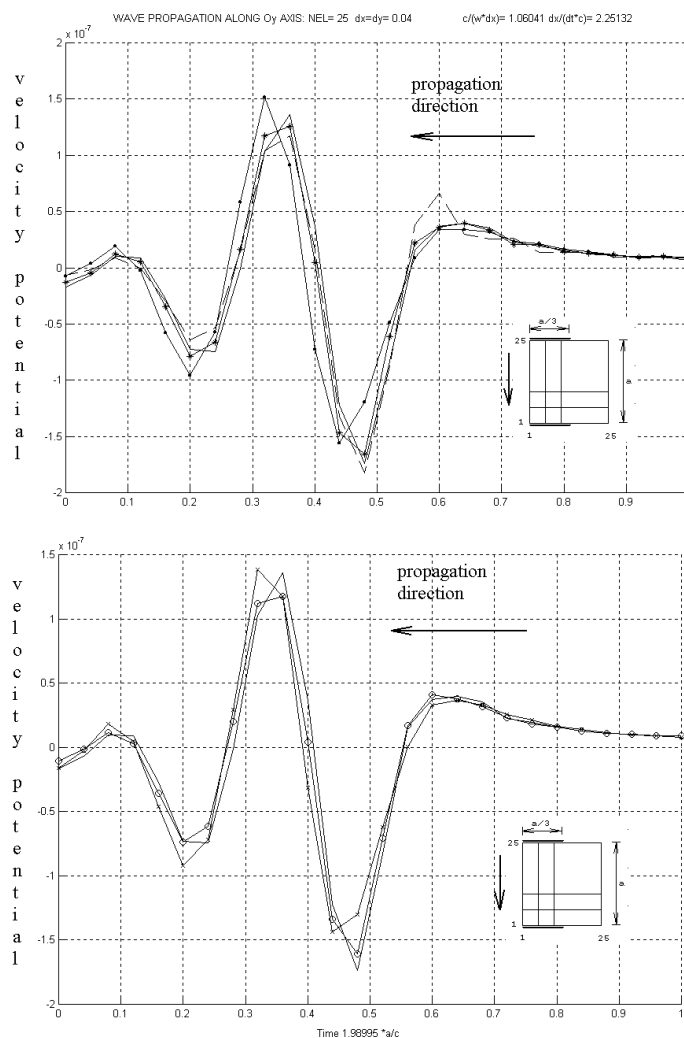


Fig.4. Shape of the wave along the left hand vertical edge at time moment $t=2a/c$ obtained by using different time integration schemes;

element size $\Delta x = \frac{c}{\omega}$; time step size $\Delta t = \frac{\Delta x}{\omega}$ within the limits of conditional stability

of integration schemes; ——— - “exact” solution; —·—·— - CDM;

----- - GNS, $\beta_0 = \frac{1}{4}$; $\beta_1 = \frac{1}{3}$; $\beta_2 = \frac{1}{2}$; $\beta_3 = 1$;

----*---- - HAM, $\lambda = \omega$; ----x---- - MTM; ----o---- - TDGFEM

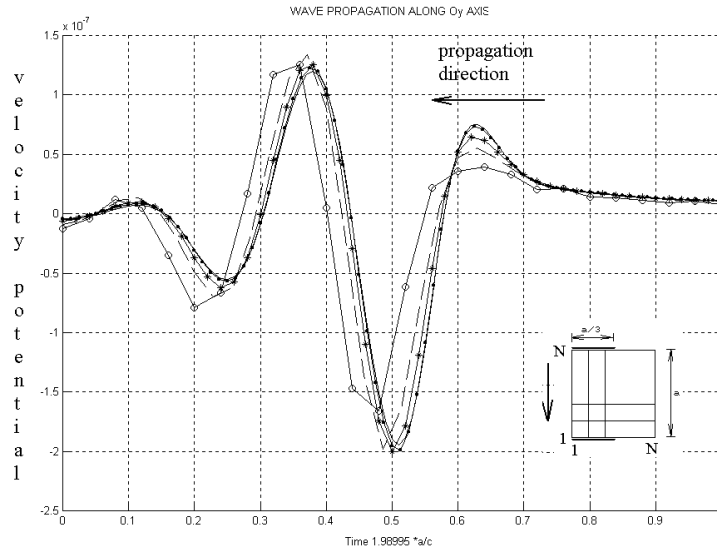


Fig.5. Shape of the wave along the left hand vertical edge at time moment $t=2a/c$ obtained by using different rectangular mesh refinement; mass matrices

$$[M^r] = 0.75[M_c^r] + 0.25[M_f^r];$$

$$\text{———} - N=101, \text{ element size } \Delta x = \frac{c}{4.25\omega}; \quad \text{— — —} - N=81, \text{ element size } \Delta x = \frac{c}{3.4\omega};$$

$$\text{---*---} - N=51, \text{ element size } \Delta x = \frac{c}{2.1\omega}; \quad \text{----} - N=36, \text{ element size}$$

$$\Delta x = \frac{c}{\omega};$$

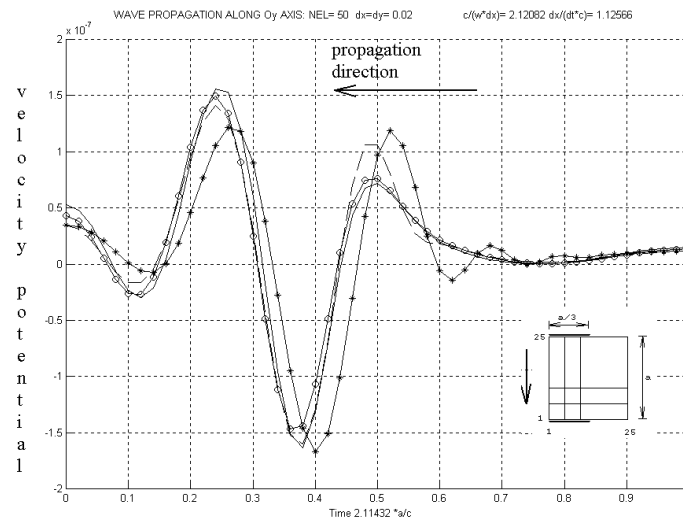


Fig.6. Shape of the wave along the left hand vertical edge at time moment $t=2.11a/c$ obtained by using different time integration schemes;

element size $\Delta x = \frac{c}{2.12\omega}$; time step size $\Delta t = \frac{\Delta x}{\omega}$ requires the unconditional stability of integration schemes;

——— - "exact" solution

---*--- - GNS, $\beta_0 = \frac{1}{2}$; $\beta_1 = \frac{1}{2}$; $\beta_2 = 1$;

----- - HAM, $\lambda = \omega$; ---o--- - TDGFEM

4 Computer program for explicit analysis of elastic and acoustic ultrasonic wave propagation

In order to develop a computer program able to perform explicit analysis of ultrasonic pulse propagation problems in real specimens an efficient computational strategy has been employed.

(a) Large domains under investigation are subdivided into rectangular areas of uniform quadrilateral finite element meshes and small number of areas of arbitrary geometrical shape presented by free meshes. The product $[\mathbf{K}]\{U_i\}$ for the regular domains is being obtained on the element level and then assembled to nodal vector. As all the matrices of the elements in this domain are identical, the calculation of the product corresponding to node ij , can be presented by the recursive formula as

$$\begin{aligned} [\mathbf{K}]\{U\}_{ij} = & \left([\mathbf{K}_{11}^e] + [\mathbf{K}_{22}^e] + [\mathbf{K}_{33}^e] + [\mathbf{K}_{44}^e] \right) \{U\}_{ij} + \left([\mathbf{K}_{21}^e] + [\mathbf{K}_{34}^e] \right) \{U\}_{i-1,j} + \left([\mathbf{K}_{23}^e] + [\mathbf{K}_{14}^e] \right) \{U\}_{i,j+1} + \\ & + \left([\mathbf{K}_{12}^e] + [\mathbf{K}_{43}^e] \right) \{U\}_{i+1,j} + \left([\mathbf{K}_{41}^e] + [\mathbf{K}_{32}^e] \right) \{U\}_{i,j-1} + \\ & + [\mathbf{K}_{24}^e] \{U\}_{i-1,j+1} + [\mathbf{K}_{13}^e] \{U\}_{i+1,j+1} + [\mathbf{K}_{42}^e] \{U\}_{i+1,j-1} + [\mathbf{K}_{31}^e] \{U\}_{i-1,j-1} \end{aligned} \quad (5)$$

where $[\mathbf{K}_{st}^e]$, $s, t = 1, 2, 3, 4$ are blocks of dimension 2×2 of the stiffness matrix of the quadrilateral element the local nodal numbers of which are being assigned from the bottom left corner in counter-clockwise direction.

Formula (5) recalls the relations of the finite difference method described in [2] invoking similar number of arithmetic operations to be performed during each time integration step. However, the finite element approach avoids algorithmic difficulties encountered when the finite difference model has to be connected with adjacent regions of arbitrary shape modelled by free finite element meshes. The calculation of the displacements for free-meshed domains requires considerably greater amounts of computational time pro node, however, usually the number of nodes in such domains is small in comparison with the total number of nodes of the model. Diagonal (lumped) mass and damping matrices are being used, therefore no matrix inverses are necessary in (2).

(b) The domain regularly meshed by quadrilateral elements is subdivided into rectangular subdomains displacements of which are stored as files on hard disc. For each subdomain the activity index is supplied indicating if the wave has reached the subdomain. Inactive subdomains are excluded from computation of $[\mathbf{K}]\{U_i\}$ and considerable time saving is achieved during first stages of the wave propagation. Similarly, the subdomains passed by the wave and containing only very small residual vibration are indicated as inactive and excluded from computation until they are reached by the next wavefront. The velocity of the excited wave propagation do not coincides with the rate at which the induced signal propagates in the finite element mesh. At the next time integration step non zero displacement value attains

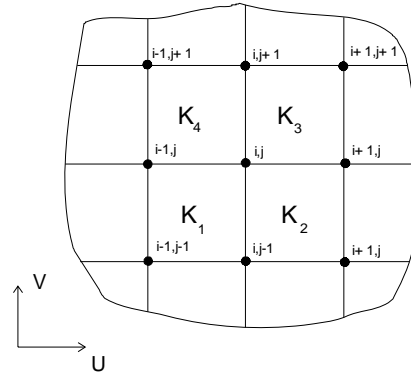


Fig. 7 Fragment of the regular meshing zone

nodes which surround node had started to vibrate at previous time step, thus the signal propagating rate in the mesh is $\frac{\Delta x}{\Delta t}$. It is at least 2 times greater than actual velocity of the longitudinal wave. It is possible to reduce excitation rate by setting bigger time step, however that forces to utilize an unconditionally stable time integration algorithm. The proposed technique by means of filtrating allows eliminate the numerical noise which propagates with greater speed than the longitudinal wave. Displacements of the nodes are being set to zero value if they do not exceed a predefined threshold. Actually it is sufficient to nullify all the values below the $10^{-4} \times u_{\max}$, where u_{\max} corresponds to the maximum value of the displacement since the start of program. Such checks of displacement values is being performed after every time integration step.

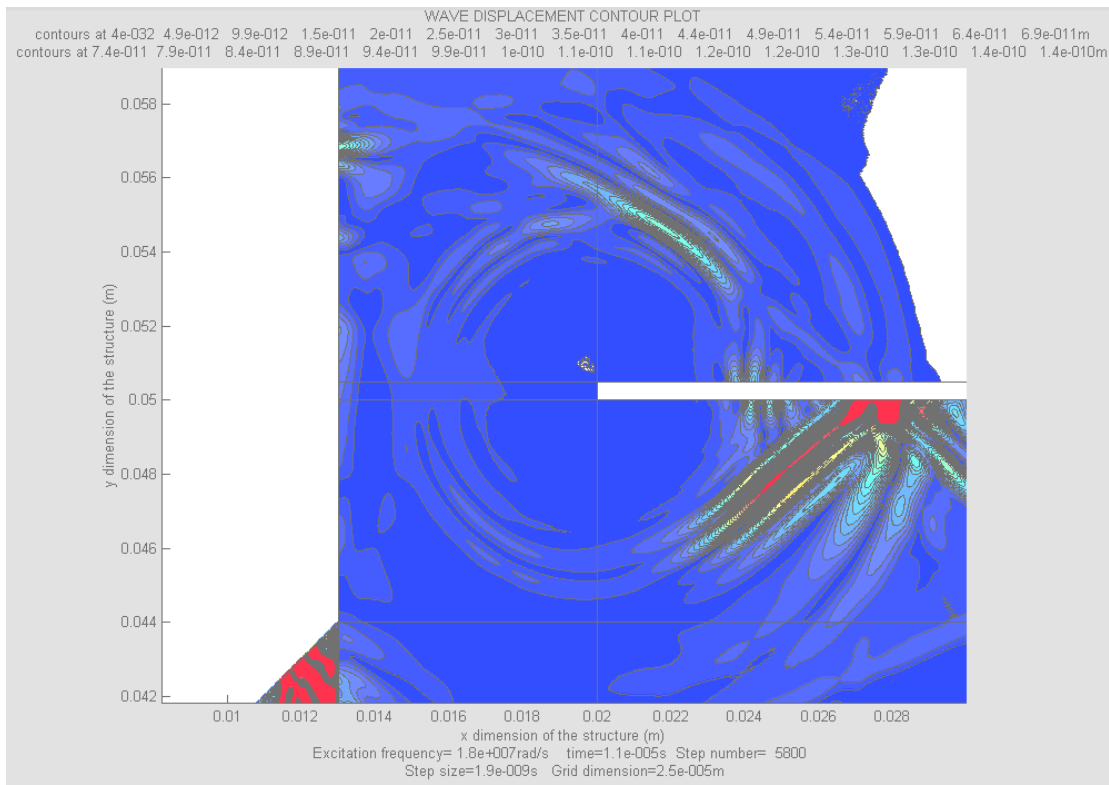


Fig.8. A fragment of elastic domain: the displacement contour plot of the ultrasonic pulse refraction and diffraction view from the edges of an internal defect(gap). The computation performed on a PC; total number of elements of the model about 4,000,000.

(c) Products $[K]\{U_i\}$ could be evaluated for every individual rectangular zone by using displacements of certain and adjacent zones. If mass matrices are diagonal, formula (5) can be used for every zone separately. That allows to store in the random access memory only products $[K]\{U_i\}$ corresponding to the nodes shared by adjacent areas while products $[K]\{U_i\}$ corresponding to the internal nodes of the area are stored on a hard disc.

(d) Wave formations of small amplitudes the development of which is of no interest in the future can be eliminated by establishing the zero threshold value for displacements. The displacement values of the whole model are modified at time steps t and $t-h$ as follows:

$$u_i = \begin{cases} \text{sign}(u_i) \times (|u_i| - u_{crit}) \times \frac{u_{max}}{u_{max} - u_{crit}}, & \text{jeigu } |u_i| - u_{crit} > 0 ; \\ 0, & \text{jeigu } |u_i| - u_{crit} \leq 0 \end{cases} \quad (6)$$

The computer program has been developed in Compaq FORTRAN and run on a Pentium computer. The displacement contour plot on Fig.8 presents a wave pattern obtained as a result of a 3MHz ultrasonic pulse sent into 8x15cm steel plate through an oblique plexyglass cone.

5 Conclusions

During the finite element modelling of the transient ultrasonic pulse propagation the main challenge is the computational performance of the model expressed in terms of amount of memory and computation time. It is reasonable to keep the mesh and time step sizes of the model as large as possible ensuring simultaneously the accuracy of computation.

- the accuracy of natural frequencies of the region that finally determine the dispersion relation of the model can be significantly improved by using mass matrices in the form of linear combination of lumped and consistent ones. This enables to keep the element linear dimension up to 3 times larger compared with element sizes necessary in the case of lumped mass matrices and comprise about 7-8 elements per wavelength of the main harmonic component of the typical pulse. The highest harmonic component of the pulse has about 2.5 times greater frequency. The price for such an improvement is a non-diagonal form of the mass matrix, however, employing iterative algebraic equation solvers requires only about 7 iterations at each time step;
- larger elements allow to use greater time steps of time integration. In coarser meshes the accuracy and not the algorithmic stability requirements predetermine the time step size. Among five different time integration algorithms under consideration the 3rd order maximum accuracy generalized Newmark's scheme gives the best results when integrating the ultrasonic pulse propagation equations requiring about 15 time steps per one period of the main harmonic component of the typical pulse. Similar accuracy has been obtained by using the time discontinuous Galerkin finite element method, however, the generalized Newmark's scheme requires less computational time;
- in the case of more refined meshes the 15 time steps per one period of the main harmonic component of the typical pulse requires unconditional stability of the numerical integration scheme. The time discontinuous Galerkin finite element method gave the best results in this case. It is important to have efficient procedure to solve the algebraic equations and to perform the necessary iteration at each time step having in mind that practical problems are too large to perform the triangularization of the matrix.

References

- [1] R.S.Shechter, H.H.Chaskelis, R.B.Mignona, P.P.Delsanto, Real-Time Parallel Computation and Visualization of Ultrasonic Pulses in Solids, *Science*, **265**, 1188-1192.
- [2] K.Harumi, 'Computer simulation of ultrasonics in a solid', *NDT International*, **19**,N.5, 315-332, (1986).
- [3] M.J.Bluck and S.P.Walker, Analysis of three-dimensional transient acoustic wave propagation using the boundary integral equation method, *Int. J. Num. Meth. Eng.*, **39**, 1419-1431, (1996).
- [4] V.Suchivoraphanphong, S.P.Walker, M.J.Bluck, Extending integral equation time domain acoustic scattering analysis to larger problems, *Int. J. Num. Meth. Eng.*, **46**, 1997-2010, (1999).
- [5] S.Han and Y.Ichikawa, Numerical modelling for scattering of waves in three dimensional cracked material, *Int. J. Num. Meth. Eng.*, **38**, 4081-4100, (1995).
- [6] V.Daniulaitis and R.Barauskas, Modelling techniques for ultrasonic wave propagation in Solids, *Ultragarsas*, N1(29),(1998).
- [7] V.Daniulaitis and R.Barauskas, Modelling techniques for ultrasonic wave propagation in solids:2D case, *Ultragarsas*, N2(30),7-10,(1998).
- [8] P. Morse, H.Feshbach, *Methods of Theoretical Physics*, Parts I&II, McGraw-Hill, New-York,(1953).
- [9] O.Zienkiewicz, *The Finite Element Method, IV edition*, Volumes I&II, McGraw-Hill, London, (1989).
- [10] K.J.Bathe, *Finite Element procedures in Finite Element Analysis*, Prentice Hall, Englewood Cliffs, N.J.,(1987).
- [11] Katona, O.C.Zienkiewicz,'A unified set of single step algorithms, Part 3: the beta-*m* method, a generalization of the Newmark's scheme', *Int. J. Num. Meth. Eng.*, **21**, 1345-1359, (1985).
- [12] I.Senjanovic, Harmonic acceleration method for dynamic structural analysis, *Comp.Struct.*, **18**, N.1, 71-80, (1984).
- [13] S.Pezeshk and C.V.Camp, An explicit time integration technique for dynamic analyses, *Int. J. Num. Meth. Eng.*, **38**, 2265-2281, (1995).
- [14] X.D.Li and N.-E.Wiberg, Structural dynamic analysis by a time-discontinuous Galerkin finite element method, *Int. J. Num. Meth. Eng.*, **39**, 2131-2152, (1996).